

Nonlinear thermoelastic analysis of FGM thick plates

Malika Bouhlali¹, Abdelbaki Chikh^{1,2}, Mohammed Bouremana¹,
Abdelhakim Kaci^{1,3}, Fouad Bourada^{1,4}, Khalil Belakhdar^{1,5}
and Abdelouahed Tounsi^{*1,6}

¹Department of Civil Engineering, Faculty of Technology,
Material and Hydrology Laboratory, University of Sidi Bel Abbes, Algeria

²Université Ibn Khaldoun, BP 78 Zaaroura, 14000 Tiaret, Algeria

³Department of Civil Engineering and Hydraulics, University of Saida, Algeria

⁴Department of Science and Technology, University Centre of Tissemsilt,
BP 38004 Ben Hamouda, Algeria

⁵Department of Science and Technology, University Centre of Tamanrasset, BP 10034 Sersouf,
Tamanrasset, Algeria

⁶Department of Civil and Environmental Engineering,
King Fahd University of Petroleum & Minerals, Dhahran, Saudi Arabia

(Received July 1, 2019, Revised September 29, 2019, Accepted October 5, 2019)

Abstract. In this paper, a new application of a four variable refined plate theory to analyze the nonlinear bending of functionally graded plates exposed to thermo-mechanical loadings, is presented. This recent theory is based on the assumption that the transverse displacements consist of bending and shear components in which the bending components do not contribute toward shear forces, and similarly, the shear components do not contribute toward bending moments. The derived transverse shear strains has a quadratic variation across the thickness that satisfies the zero traction boundary conditions on the top and bottom surfaces of the plate without using shear correction factors. The material properties are assumed to vary continuously through the thickness of the plate according to a power-law distribution of the volume fraction of the constituents. The solutions are achieved by minimizing the total potential energy. The non-linear strain–displacement relations in the von Karman sense are used to derive the effect of geometric non-linearity. It is concluded that the proposed theory is accurate and simple in solving the nonlinear bending behavior of functionally graded plates.

Keywords: functional composites; plate; large deformation; energy method; thermo-mechanical loading

1. Introduction

Functionally graded materials (FGM) are a class of composites in which the properties of the material gradually change over one or more Cartesian directions. A typical FGM plate considers a continuous variation of material properties over the thickness direction by mixing two different materials (Miyamoto *et al.* 1999). The gradual variation of properties avoids the delaminating type

*Corresponding author, Professor, E-mail: tou_abdel@yahoo.com

failure that is common in laminated composites. The FGM concept has many applications in several fields such as aerospace and civil (Miyamoto *et al.* 1999, Sobhy 2013, Eltaher 2013, Ahmed 2014, Kar and Panda 2015, Hadji *et al.* 2016, Kar and Panda 2016ab, Akbaş 2017, Akavci 2016, Aldousari 2017, Avcar and Alwan 2017, Civalek 2017, Shahsavari *et al.* 2018, Ghayesh and Farokhi, 2018, Avcar and Mohammed 2018, Bensaid *et al.* 2018, Avcar 2019, Mohammadzadeh *et al.* 2019). The increase of FGM applications requires accurate plate theories with more realistic assumptions. Typically, the analysis of FGM plates is performed using the first-order shear deformation theory (FSDT) (Thai and Choi 2013) or higher-order shear deformation theories (HSDT), Mantari *et al.* 2011, Thai and Kim 2013, Siddiqui 2015, Kolahchi *et al.*, 2017). The FSDT gives acceptable results but depends on the shear correction factor which is hard to find since it depends on many parameters. Although the HSDT with five unknowns are sufficiently accurate to predict response of thin to thick plate without the need of a shear correction factor, their equations of motion are much more complicated than those of FSDT and classical plate theory (CPT).

A new four variable refined plate theory is developed recently to study the static and the free vibration behavior of FGM plate. This new refined plate theory is based on the assumption that the in-plane and transverse displacements consist of bending and shear components. Noting that, the bending components do not contribute toward shear forces and, likewise, the shear components do not contribute toward bending moments. The most interesting feature of this theory is that the resulting transverse shear strains has a quadratic variation across the thickness with zero traction boundary conditions on the top and bottom surfaces of the plate without using shear correction factors. In addition, it has strong similarities with the classical plate theory (CPT) in some aspects such as governing equation, boundary conditions and moment expressions.

It should be noted that recently, the refined theory become more and more popular since it simplify the solution by reducing the number of the required unknown variables. This theory has been used to solve different mechanical and thermal FGM plates problems (Nguyen-Xuan *et al.* 2014, Nguyen-Xuan *et al.* (2014)). Although several studies on the nonlinear bending behavior of functionally graded plates have been carried out based on variety of plate theories, only few studies are conducted to study the nonlinear bending behavior of FGM plates using the refined plate theory. Therefore, the aim of this study is to extend this new refined theory to the analysis of the nonlinear bending behavior of FGM plates.

Kaci and his co-authors (Bakhti *et al.* 2013, Kaci *et al.* 2014, 2013a, b and 2014) presented many pieces of research work where they studied the nonlinear bending behavior of simply-supported FG plate subjected to the action of mechanical loads based on the refined plate theory. Nguyen-Xuan *et al.* (2014) presented isogeometric finite element approach with a refined plate theory to carry out static, vibration and buckling analyze FGM plates. Also, and his co-authors carried out an Isogeometric analysis of FGM plates where their solution is based on a new quasi-3D shear deformation theory with adopting the physical neutral surface as a reference. Li *et al.* (2017) studied the thermomechanical bending behavior of sandwich plates using a four-variable refined theory. Another refined theories based on non-polynomial kinematics is presented by Ramos *et al.* (2016) to study simply supported sandwich FGM plates under linear and nonlinear thermal loading. In their paper, Tornabene *et al.* (2016) compared the vibration characteristics numerical 2D of cylindrical bending models of FGM plats using finite element method versus 3D exact model.

The primary objective of this paper is to present a general formulation for functionally graded plates using the third-order shear deformation plate theory with only four variables instead

of five variables and developing the concept of minimal energy method for analysis FGM thick plates for simply supported plates based on the third-order theory and non-linear static that accounts for the thermo-mechanical coupling and geometric non-linearity. To make the study reasonably complete, numerical results of the linear and linear theory are also presented.

2. Theoretical formulation

2.1 Displacement field and strains

Consider an elastic plate occupying the region $[0,a] \times [0,b] \times [-h/2, h/2]$ in rectangular Cartesian coordinates (x, y, z) . The mid-plane of the plate is defined by $z=0$ and its external bounding planes being defined by $z=\pm h/2$, as shown in Fig. 1. The top and bottom layers of the plate are made of an isotropic material with material properties varying smoothly in the z (thickness) direction only. Hence, the following displacement field is assumed

$$\begin{cases} u(x, y, z) = u_0(x, y) - z \frac{\partial w_b}{\partial x} - f(z) \frac{\partial w_s}{\partial x} \\ v(x, y, z) = v_0(x, y) - z \frac{\partial w_b}{\partial y} - f(z) \frac{\partial w_s}{\partial y} \\ w(x, y, z) = w_b(x, y) + w_s(x, y) \end{cases} \quad (1)$$

The function $f(z)$ is chosen in the following form

$$f(z) = z - \frac{h}{\pi} \sin\left(\frac{\pi}{h} z\right) \quad (2)$$

where u_0 and v_0 are corresponding displacements of a point along the mid plane; w_b and w_s are the bending and shear components of transverse displacement, respectively.

The non-linear von Karman strain–displacement relationship is as follows

$$\begin{cases} \varepsilon_x = \frac{\partial u}{\partial x} + \frac{1}{2} \left(\frac{\partial w_b}{\partial x} + \frac{\partial w_s}{\partial x} \right)^2 \\ \varepsilon_y = \frac{\partial v}{\partial y} + \frac{1}{2} \left(\frac{\partial w_b}{\partial y} + \frac{\partial w_s}{\partial y} \right)^2 \\ \varepsilon_z = \frac{\partial w_b}{\partial z} + \frac{\partial w_s}{\partial z} = 0 \\ \gamma_{xy} = \frac{\partial v}{\partial x} + \frac{\partial u}{\partial y} + \left(\frac{\partial w_b}{\partial x} + \frac{\partial w_s}{\partial x} \right) \left(\frac{\partial w_b}{\partial y} + \frac{\partial w_s}{\partial y} \right) \\ \gamma_{yz} = \frac{\partial v}{\partial z} + \left(\frac{\partial w_b}{\partial y} + \frac{\partial w_s}{\partial y} \right) \\ \gamma_{xz} = \frac{\partial u}{\partial z} + \left(\frac{\partial w_b}{\partial x} + \frac{\partial w_s}{\partial x} \right) \end{cases} \quad (3)$$

On the basis of the displacement field given in Eq. (1), Eq. (3) becomes

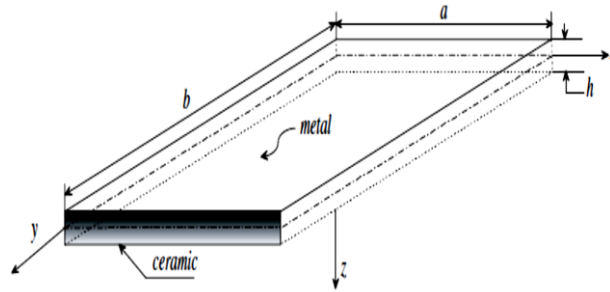


Fig. 1 Geometry and dimensions of the plate

$$\begin{cases} \varepsilon_x = \varepsilon_x^0 + z k_x^b + f(z) k_x^s \\ \varepsilon_y = \varepsilon_y^0 + z k_y^b + f(z) k_y^s \\ \gamma_{xy} = \gamma_{xy}^0 + z k_{xy}^b + f(z) k_{xy}^s \\ \gamma_{yz} = g(z) \gamma_{yz}^s \\ \gamma_{xz} = g(z) \gamma_{xz}^s \\ \varepsilon_z = 0 \end{cases} \quad (4)$$

$$\begin{aligned} \varepsilon_x^0 &= \frac{\partial u_0}{\partial x} + \frac{1}{2} \left(\frac{\partial w_b}{\partial x} + \frac{\partial w_i}{\partial x} \right)^2, & k_x^b &= -\frac{\partial^2 w_b}{\partial x^2}, \\ k_x^s &= -\frac{\partial^2 w_i}{\partial x^2}, & \varepsilon_y^0 &= \frac{\partial v_0}{\partial y} + \frac{1}{2} \left(\frac{\partial w_b}{\partial y} + \frac{\partial w_i}{\partial y} \right), \\ k_y^b &= -\frac{\partial^2 w_b}{\partial y^2}, & k_y^s &= -\frac{\partial^2 w_i}{\partial y^2}, \\ \gamma_{xy}^0 &= \frac{\partial v_0}{\partial x} + \frac{\partial u_0}{\partial y} + \left(\frac{\partial w_b}{\partial x} + \frac{\partial w_i}{\partial x} \right) \left(\frac{\partial w_b}{\partial y} + \frac{\partial w_i}{\partial y} \right), & & \\ k_{xy}^b &= -2 \frac{\partial^2 w_b}{\partial x \partial y}, & k_{xy}^s &= -2 \frac{\partial^2 w_i}{\partial x \partial y}. \end{aligned} \quad (5)$$

$$\gamma_{yz}^s = \frac{\partial w_i}{\partial y}, \gamma_{xz}^s = \frac{\partial w_i}{\partial x}, \quad g(z) = 1 - f'(z), \quad f'(z) = \frac{df(z)}{dz}$$

2.2 Constitutive equations

Consider a FG plate made of two constituent functionally graded materials, the material properties of the plate such as Young’s modulus E , the coefficient of thermal conductivity k , the coefficient of thermal expansion α are considered to change continuously across the thickness by power law are given by the rule of mixtures as

$$\begin{aligned} E(z) &= (E_c - E_m) V_c + E_m \\ \kappa(z) &= (\kappa_c - \kappa_m) V_c + \kappa_m \\ \alpha(z) &= (\alpha_c - \alpha_m) V_c + \alpha_m \end{aligned} \quad (6)$$

where $V_c = (0.5 + z/h)^n$ is the volume fraction of ceramic, the subscripts c and m refer to ceramic and metal, respectively and $n(0 \leq n < \infty)$ is the gradient index indicating the volume fraction of material.

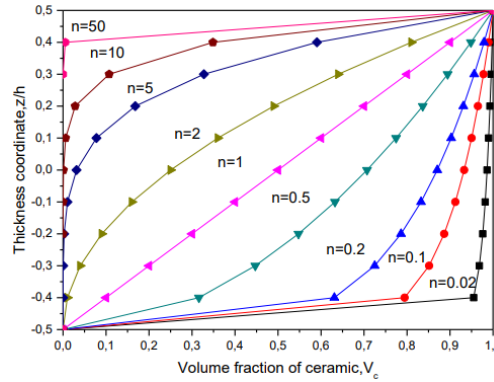


Fig. 2 Variation of volume fraction of ceramic V_c through the thickness of a FG plate for various gradient indexes n

The variation of the volume fraction of ceramic V_c across the thickness of the plate is plotted in Fig. 2 for various values of the power law index.

The linear thermo-elastic constitutive relations of an isotropic material are given by

$$\begin{Bmatrix} \sigma_x \\ \sigma_y \\ \sigma_{xy} \\ \sigma_{yz} \\ \sigma_{xz} \end{Bmatrix} = \begin{bmatrix} Q_{11} & Q_{12} & 0 & 0 & 0 \\ Q_{12} & Q_{22} & 0 & 0 & 0 \\ 0 & 0 & Q_{66} & 0 & 0 \\ 0 & 0 & 0 & Q_{44} & 0 \\ 0 & 0 & 0 & 0 & Q_{55} \end{bmatrix} \begin{Bmatrix} \varepsilon_x \\ \varepsilon_y \\ \gamma_{xy} \\ \gamma_{yz} \\ \gamma_{xz} \end{Bmatrix} = \begin{Bmatrix} 1 \\ 1 \\ 0 \\ 0 \\ 0 \end{Bmatrix} \alpha \Delta T \quad (7)$$

where

$$Q_{11} = Q_{22} = \frac{E(z)}{1-\nu^2}, Q_{12} = \nu Q_{11}, Q_{44} = Q_{55} = Q_{66} = \frac{E(z)}{2(1+\nu)} \quad (8)$$

and ΔT is the temperature change from a stress-free state.

2.3 Equations of motion

The equilibrium equations associated with the present shear deformation theory are

$$\begin{cases} \delta u_0 : \frac{\partial N_x}{\partial x} + \frac{\partial N_{xy}}{\partial y} = 0 \\ \delta v_0 : \frac{\partial N_{xy}}{\partial x} + \frac{\partial N_y}{\partial y} = 0 \\ \delta w_b : \frac{\partial^2 M_x^b}{\partial x^2} + 2 \frac{\partial^2 M_{xy}^b}{\partial x \partial y} + \frac{\partial^2 M_y^b}{\partial y^2} + \bar{N} + q(x) = 0 \\ \delta w_s : \frac{\partial^2 M_x^s}{\partial x^2} + 2 \frac{\partial^2 M_{xy}^s}{\partial x \partial y} + \frac{\partial^2 M_y^s}{\partial y^2} + \frac{\partial S_{xz}^s}{\partial x} + \frac{\partial S_{yz}^s}{\partial y} + \bar{N} + q(x) = 0 \end{cases} \quad (9)$$

with

$$\begin{aligned} \bar{N} = & \frac{\partial}{\partial x} \left[N_x \frac{\partial(w_b + w_s)}{\partial x} + N_{xy} \frac{\partial(w_b + w_s)}{\partial y} \right] + \\ & \frac{\partial}{\partial y} \left[N_{xy} \frac{\partial(w_b + w_s)}{\partial x} + N_y \frac{\partial(w_b + w_s)}{\partial y} \right] \end{aligned} \quad (10)$$

where $q(x)$ is the transverse load on the top surface of the plate.

In Eq. (9), the generalized stress resultants are defined as

$$\begin{aligned} \begin{Bmatrix} N_x & N_y & N_{xy} \\ M_x^b & M_y^b & M_{xy}^b \\ M_x^s & M_y^s & M_{xy}^s \end{Bmatrix} &= \int_{-h/2}^{h/2} (\sigma_x, \sigma_y, \tau_{xy}) \begin{Bmatrix} 1 \\ z \\ f(z) \end{Bmatrix} dz \\ (S_x^s, S_y^s) &= \int_{-h/2}^{h/2} (\tau_{xz}, \tau_{yz}) g(z) dz \end{aligned} \tag{11}$$

Using Eq. (7) in Eqs. (11), the stress resultants of a plate can be related to the total strains by

$$\begin{Bmatrix} N \\ M^b \\ M^s \end{Bmatrix} = \begin{bmatrix} A & B & B^T \\ A & D & D^s \\ B^T & D^s & H^s \end{bmatrix} \begin{Bmatrix} \varepsilon \\ k^b \\ k^s \end{Bmatrix} = \begin{Bmatrix} N^T \\ M^{bT} \\ M^{sT} \end{Bmatrix} \quad S = A^s \gamma \tag{12}$$

where

$$\begin{aligned} N &= \{N_x, N_y, N_{xy}\}^T; M^b = \{M_x^b, M_y^b, M_{xy}^b\}^T \\ M^s &= \{M_x^s, M_y^s, M_{xy}^s\}^T; N^T = \{N_x^T, N_y^T, 0\}^T \\ M^{bT} &= \{M_x^{bT}, M_y^{bT}, 0\}^T; M^{sT} = \{M_x^{sT}, M_y^{sT}, 0\}^T \\ \varepsilon &= \{\varepsilon_x^0, \varepsilon_y^0, \gamma_{xy}^0\}^T; k^b = \{k_x^b, k_y^b, k_{xy}^b\}^T; k^s = \{k_x^s, k_y^s, k_{xy}^s\}^T \\ A &= \begin{bmatrix} A_{11} & A_{12} & 0 \\ A_{12} & A_{22} & 0 \\ 0 & 0 & A_{66} \end{bmatrix}, \quad B = \begin{bmatrix} B_{11} & B_{12} & 0 \\ B_{12} & B_{22} & 0 \\ 0 & 0 & B_{66} \end{bmatrix}, \\ D &= \begin{bmatrix} D_{11} & D_{12} & 0 \\ D_{12} & D_{22} & 0 \\ 0 & 0 & D_{66} \end{bmatrix}, \quad B^s = \begin{bmatrix} B_{11}^s & B_{12}^s & 0 \\ B_{12}^s & B_{22}^s & 0 \\ 0 & 0 & B_{66}^s \end{bmatrix} \\ D^s &= \begin{bmatrix} D_{11}^s & D_{12}^s & 0 \\ D_{12}^s & D_{22}^s & 0 \\ 0 & 0 & D_{66}^s \end{bmatrix}, \quad H^s = \begin{bmatrix} H_{11}^s & H_{12}^s & 0 \\ H_{12}^s & H_{22}^s & 0 \\ 0 & 0 & H_{66}^s \end{bmatrix} \\ S &= \{S_x^s, S_y^s\}^T, \quad \gamma = \{\gamma_{xz}, \gamma_{yz}\}^T, \quad A^s = \begin{bmatrix} A_{44}^s & 0 \\ 0 & A_{55}^s \end{bmatrix} \end{aligned} \tag{13}$$

where A_{ij}, B_{ij} , etc., are the plate stiffness, defined by

$$\begin{aligned} \begin{Bmatrix} A_{11} & B_{11} & D_{11} & B_{11}^s & D_{11}^s & H_{11}^s \\ A_{12} & B_{12} & D_{12} & B_{12}^s & D_{12}^s & H_{12}^s \\ A_{66} & B_{66} & D_{66} & B_{66}^s & D_{66}^s & H_{66}^s \end{Bmatrix} &= \int_{-h/2}^{h/2} Q_{11} \begin{Bmatrix} 1, z, z^2, f(z), z f(z), f^2(z) \end{Bmatrix} \begin{Bmatrix} 1 \\ \nu \\ \frac{1-\nu}{2} \end{Bmatrix} dz \\ & \begin{pmatrix} A_{22} \\ B_{22} \\ D_{22} \\ B_{22}^s \\ D_{22}^s \\ H_{22}^s \end{pmatrix} = \begin{pmatrix} A_{11} \\ B_{11} \\ D_{11} \\ B_{11}^s \\ D_{11}^s \\ H_{11}^s \end{pmatrix} \end{aligned} \tag{14}$$

and

$$A_{44}^* = A_{55}^* = \int_{-h/2}^{h/2} \frac{E(z)}{2(1+\nu)} [g(z)]^2 dz, \tag{14}$$

The stress and moment resultants, $N_x^T = N_y^T$, $M_x^{bT} = M_y^{bT}$ and $M_x^{sT} = M_y^{sT}$ due to thermal loading are defined respectively by

$$\begin{Bmatrix} N_x^T \\ M_x^{bT} \\ M_x^{sT} \end{Bmatrix} = \int_{-h/2}^{h/2} \frac{E(z)}{1-\nu} \alpha(z) \Delta T \begin{Bmatrix} 1 \\ z \\ f(z) \end{Bmatrix} dz \tag{15}$$

2.3 Thermal analysis

It is assumed that the temperature varies only in the thickness direction and constant at the ceramic and metal rich surfaces. The one dimensional steady-state heat conduction equation in the z-direction is given by

$$-\frac{d}{dz} \left(\kappa(z) \frac{dT(z)}{dz} \right) = 0 \tag{16}$$

Here a stress-free state is assumed to exist at $T_0=25^\circ\text{C}$. The thermal conductivity coefficient $k(z)$ is assumed to follow the power-law relation in Eq. (5).

By using the boundary conditions $T(h/2)=T_c$ and $T(-h/2)=T_m$, and separating the variables in Eq. (16) and substituting for $\kappa(z)$ yields

$$dT = C_{1n} \frac{dz}{\Delta\kappa \left((1/2) - (z/h) \right)^n + \kappa_c} \tag{17}$$

where $\Delta\kappa=k_m-k_c$.

Then, the following variables are introduced

$$\mu^n = \frac{k_c}{\Delta\kappa} \quad \text{and} \quad \xi = \frac{1}{2} - \frac{z}{h} \tag{18}$$

Substituting Eq. (18) into Eq. (17) and integrating the result yields

$$T(\xi) = -C_{1n} \frac{h}{\Delta\kappa} \int \frac{d\xi}{\xi^n + \mu^n} + C_{2n} \tag{19}$$

Noting that, the exact solution of the integral in Eq. (18) is evaluated by Tuma (1970) for $n=0.5$ and integer values of n . Accordingly, by using the solution of Eq. (18) in Eq. (16) for $n=0, 0.5$ and integer values of n , we find

$$T(z) = -C_{1n} \frac{h}{\Delta\kappa} A_n(z) + C_{2n} \tag{20}$$

where C_{1n} and C_{2n} are simply evaluated by applying the appropriate thermal boundary conditions on the top and bottom surfaces of the plate. So, we get

$$C_{1n} = -\frac{(T_c - T_m)\Delta k}{h[A_n(h/2) - A_n(-h/2)]}, \text{ and } C_{2n} = \frac{T_m A_n(h/2) - T_c A_n(-h/2)}{[A_n(h/2) - A_n(-h/2)]} \tag{21}$$

with

$$A_0(z) = \frac{\Delta k}{k_m} \left(\frac{1}{2} - \frac{z}{h} \right) \quad A_{1/2}(z) = 2\sqrt{\frac{1}{2} - \frac{z}{h}} - 2\frac{k_c}{\Delta k} L_n \left(\sqrt{\frac{1}{2} - \frac{z}{h}} + \frac{k_c}{\Delta k} \right) \tag{22}$$

Also for the integer values of n the quantity A_n appearing in Eq. (20) is given by

$$\begin{aligned} A_n(z) = & \frac{2}{n(k_c / \Delta k)^{(n-1)/n}} \sum_{i=1}^{n/2} \left[\sin \frac{(2i-1)\pi}{n} \tan^{n-1} \left(\frac{((1/2) - (z/h)) + (k_c / \Delta k)^{1/n} \cos((2i-1)\pi/n)}{(k_c / \Delta k)^{1/n} \sin((2i-1)\pi/n)} \right) \right] \\ & + \frac{1}{n(k_c / \Delta k)^{(n-1)/n}} \sum_{i=1}^{n/2} \cos \frac{(2i-1)\pi}{n} L_n \left[\left(\frac{1}{2} - \frac{z}{h} \right)^2 \right] \\ & + 2 \left(\frac{k_c}{\Delta k} \right)^{1/n} \left[\left(\frac{1}{2} - \frac{z}{h} \right) \cos \frac{(2i-1)\pi}{n} + \left(\frac{k_c}{\Delta k} \right)^{2/n} \right], \quad n = 2, 4, 6, \dots \end{aligned} \tag{23}$$

and

$$\begin{aligned} A_n(z) = & \frac{2}{n(k_c / \Delta k)^{(n-1)/n}} \sum_{i=1}^{(n-1)/2} \left[\sin \frac{2i\pi}{n} \tan^{n-1} \left(\frac{((1/2) - (z/h)) + (k_c / \Delta k)^{1/n} \cos(2i\pi/n)}{(k_c / \Delta k)^{1/n} \sin(2i\pi/n)} \right) \right] \\ & + \frac{L_n \left[((1/2) - (z/h)) + (k_c / \Delta k)^{1/n} \right]}{n(k_c / \Delta k)^{(n-1)/n}} + \frac{1}{n(k_c / \Delta k)^{(n-1)/n}} \sum_{i=1}^{(n-1)/2} \cos \frac{2i\pi}{n} L_n \left[\left(\frac{1}{2} - \frac{z}{h} \right)^2 \right] \\ & + 2 \left(\frac{k_c}{\Delta k} \right)^{1/n} \left[\left(\frac{1}{2} - \frac{z}{h} \right) \cos \frac{2i\pi}{n} + \left(\frac{k_c}{\Delta k} \right)^{2/n} \right], \quad n = 1, 3, \dots \end{aligned}$$

2.4 Solution procedure

The summation of strain energy and the change in potential energy of the uniform externally applied pressure The total potential energy (Π) of the FGM plate is determined by and is written as

$$\Pi = U + V \tag{24}$$

Here, V (the potential energy of uniform pressure) is given by

$$V = \int_0^a \int_0^b q(w_b + w_s) dx dy \tag{25}$$

with q is the uniformly distributed load. Also, the strain energy (U) is defined as

$$U = \frac{1}{2} \int_0^a \int_0^b \int_{-h/2}^{h/2} \left(\begin{aligned} & \sigma_x (\epsilon_x - \alpha(T(z) - T_0)) + \\ & \sigma_y (\epsilon_y - \alpha(T(z) - T_0)) + \\ & \tau_{xy} \gamma_{xy} + \tau_{yz} \gamma_{yz} + \tau_{xz} \gamma_{xz} \end{aligned} \right) dx dy dz \tag{26}$$

The principal of minimum potential energy is applied assuming a first guess solution for the considered displacements (i.e., u_0, v_0, w_b and w_s) over the mid-surface of the plate with considering the boundary condition for the simply supported boundaries, as

$$\left\{ \begin{array}{l} v_0(0, y) = w_b(0, y) = w_s(0, y) = \frac{\partial w_s}{\partial y}(0, y) = 0 \\ v_0(a, y) = w_b(a, y) = w_s(a, y) = \frac{\partial w_s}{\partial y}(a, y) = 0 \\ M_x^b(0, y) = M_x^s(0, y) = M_x^b(a, y) = M_x^s(a, y) = 0 \\ u_0(x, 0) = w_b(x, 0) = w_s(x, 0) = \frac{\partial w_s}{\partial x}(x, 0) = 0 \\ u_0(x, b) = w_b(x, b) = w_s(x, b) = \frac{\partial w_s}{\partial x}(x, b) = 0 \\ M_y^b(x, 0) = M_y^s(x, 0) = M_y^b(x, b) = M_y^s(x, b) = 0 \end{array} \right. \quad (27)$$

The required above fields of displacement and rotation that satisfy the simply supported boundary conditions, are defined as

$$\begin{aligned} u_0(x, y) &= C \cdot \sin\left(\frac{2\pi x}{a}\right) \sin\left(\frac{\pi y}{a}\right) \\ v_0(x, y) &= C \cdot \sin\left(\frac{\pi x}{a}\right) \sin\left(\frac{2\pi y}{a}\right) \\ w_s(x, y) &= W_0^b \cdot \sin\left(\frac{\pi x}{a}\right) \sin\left(\frac{\pi y}{a}\right) \\ w_s(x, y) &= W_0^s \cdot \sin\left(\frac{\pi x}{a}\right) \sin\left(\frac{\pi y}{a}\right) \end{aligned} \quad (28)$$

where C , W_0^b , and W_0^s are arbitrary parameters. These parameters are determined by minimizing the total potential energy as

$$\frac{\partial \Pi}{\partial (C, W_0^b, W_0^s)} = 0 \quad (29)$$

Eq. (26) yields a set of three nonlinear equilibrium equations in terms of C , W_0^b , and W_0^s . Noting that after solving these equations, the obtained constants will be used to calculate the displacements (Eq. (28)) and then the strain and stresses are found using Eq. (4) and (7).

3. Numerical results and discussion

In the present analysis, two test examples have been analyzed to ensure the accuracy and effectiveness of the present proposed method. The features of volume fraction of the ceramic phase through the dimensionless thickness direction are outlined in Figure 2. Throughout the analysis, it is assumed that the materials are perfectly elastic during the deformations. The validation and comparison of the proposed algorithm is analyzed by comparing the results with those available in the literature.

The following nondimensional parameters are introduced:

- central deflection $W=w/h$
- loading parameter $Q=qa^4/(E_m h^4)$
- axial stress $\sigma = \sigma_x h^2 / (qa^2)$, $\bar{\sigma} = 100 \sigma_x h^2 / (E_c \alpha_c T_c L^2)$
- thickness coordinate $Z=z/h$

Table 1 Nonlinear central deflection $W=w/h$ of $Si_3N_4/SUS304$ square FGM plates with varying volume fraction indexes n subjected to uniform lateral pressure

a/h	n	$q_0=4$		$q_0=8$		$q_0=12$		$q_0=16$		$q_0=20$		$q_0=40$	
		Ref ^(a)	Present										
10	0	0.1200	0.1228	0.2551	0.2325	0.3185	0.3258	0.3911	0.4047	0.4597	0.4726	0.6984	0.7152
	0.5	0.1343	0.1378	0.2421	0.2546	0.3402	0.3506	0.4189	0.4306	0.4850	0.4991	0.7471	0.7435
	1	0.1406	0.1444	0.2587	0.2646	0.3504	0.3623	0.4295	0.4435	0.4962	0.5128	0.7618	0.7604
	5	0.1552	0.1596	0.2840	0.2901	0.3814	0.3960	0.4660	0.4827	0.5399	0.5564	0.8209	0.8178
	10	0.1626	0.1671	0.2969	0.3039	0.4031	0.4129	0.4891	0.5021	0.5590	0.5775	0.8901	0.8450
20	0	0.1142	0.1179	0.2163	0.2246	0.3075	0.3162	0.3816	0.3945	0.4491	0.4622	0.6837	0.7063
	0.5	0.1283	0.1327	0.2342	0.2466	0.3303	0.3412	0.4086	0.4207	0.4751	0.4889	0.7108	0.7347
	1	0.1343	0.1390	0.2419	0.2563	0.3407	0.3527	0.4202	0.4333	0.4873	0.5024	0.7262	0.7512
	5	0.1479	0.1532	0.2730	0.2811	0.3711	0.3850	0.4560	0.4712	0.5267	0.5448	0.7818	0.8078
	10	0.1550	0.1604	0.2856	0.2941	0.3870	0.4018	0.4740	0.4907	0.5502	0.5661	0.8198	0.8343
50	0	0.1123	0.1167	0.2133	0.2225	0.3037	0.3137	0.3781	0.3918	0.4456	0.4594	0.6806	0.7037
	0.5	0.1263	0.1314	0.2315	0.2445	0.3269	0.3387	0.4051	0.4181	0.4675	0.4862	0.7807	0.7321
	1	0.1322	0.1376	0.2392	0.2541	0.3373	0.3501	0.4167	0.4306	0.4841	0.4996	0.7246	0.7485
	5	0.1455	0.1515	0.2616	0.2785	0.3675	0.3821	0.4524	0.4682	0.5236	0.5416	0.7780	0.8048
	10	0.1524	0.1587	0.2739	0.2914	0.3835	0.3989	0.4707	0.4876	0.5433	0.5630	0.8041	0.8315
100	0	0.1119	0.1165	0.2128	0.2222	0.3031	0.3133	0.3776	0.3914	0.4450	0.4590	0.6806	0.7033
	0.5	0.1259	0.1312	0.2310	0.2442	0.3263	0.3384	0.4045	0.4177	0.4670	0.4858	0.7072	0.7317
	1	0.1319	0.1374	0.2388	0.2537	0.3367	0.3497	0.4162	0.4302	0.4836	0.4992	0.7233	0.7482
	5	0.1451	0.1512	0.2611	0.2781	0.3669	0.3816	0.4518	0.4677	0.5231	0.5412	0.7782	0.8044
	10	0.1520	0.1584	0.2734	0.2910	0.3829	0.3984	0.4701	0.4872	0.5428	0.5626	0.8040	0.8311

(a) Talha and Singh (2011)

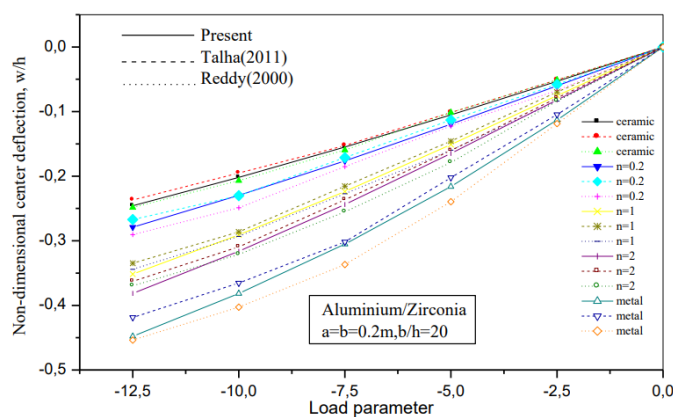


Fig. 3 Comparison of load-deflection curve for zirconia/aluminum square FGM plate subjected to uniform pressure for different theories

Example 1: In this example we consider the nonlinear bending analysis of a square FGM plate

made of silicon nitride (Si3N4) and stainless steel (SUS304), as given by Yang and Shen (2003). The top surface of the plate is ceramic-rich, whereas the bottom surface is metal-rich. The material properties are:

Metal (SUS304): $E_m=207.78$ GPa; $\nu=0.28$

Ceramic (Si3N4): $E_c=322.27$ GPa; $\nu=0.28$

Table 1 shows the nonlinear central deflection for Si3N4/SUS304 FGM square plates. The width-to-thickness ratio is taken as $a/h = 10, 20, 50$ and 100 , (i.e., ranging from thick to thin plates) and uniform lateral pressure ($q= 4, 8, 12, 20, 40$). The volume fraction index varies from $n=0$ to $n = 10$. It is realized that there is no considerable difference in central deflection observed for volume fraction index $n \geq 5$. According to Table 1 and Fig. 3, a good agreement is observed between the present solutions and the literature.

Example 2. To show the effectiveness of the minimal energy method, illustrative numerical examples of nonlinear bending behavior of FGM plate, are solved and the predicted results are compared with the existing data available in the literature.

Considering a plate composed of Aluminum and Zirconia as the respective metal and ceramic substances of a FGM which have the following material properties:

Metal (Aluminum): $E_m=70$ GPa; $\nu=0.3$; $\alpha_m=23.10^{-6}/^\circ\text{C}$; $\kappa_m=204$ W/mK.

Ceramic (Zirconia): $E_c=151$ GPa; $\nu=0.3$; $\alpha_c=10.10^{-6}/^\circ\text{C}$; $\kappa_c=2.09$ W/mK.

where the thermal load is considered as: $T_m=T_0$ and $T_c=T_0+300^\circ\text{C}$.

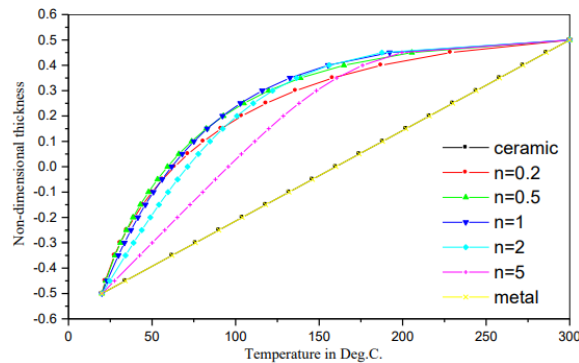


Fig. 4 Temperature profile through the thickness of aluminum-Zirconia FGM plate

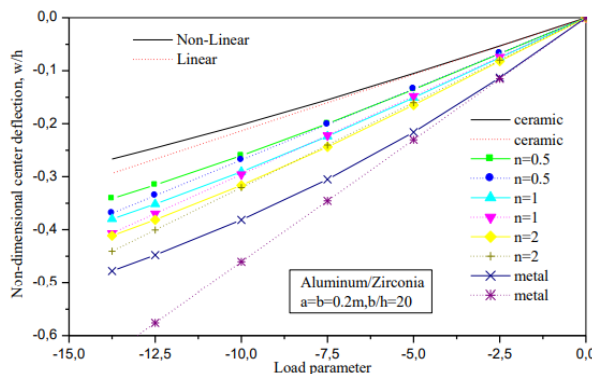


Fig. 5 Non-dimensional central deflection in terms of load parameter P in FGM plate for various values of volume fraction exponent in case of linear and nonlinear type of analysis

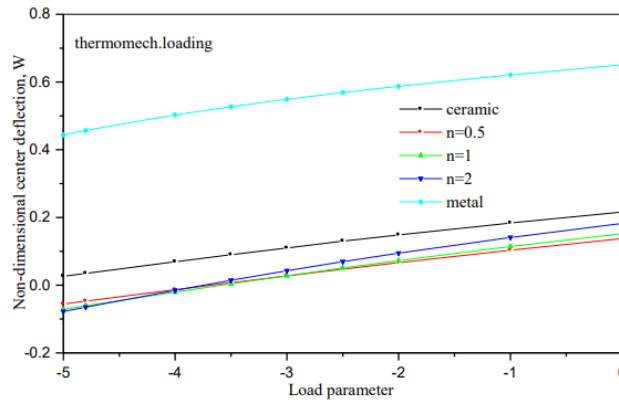


Fig. 6 Non-dimensional central deflection in terms of load parameter P for a simply supported FGM square plate under temperature field

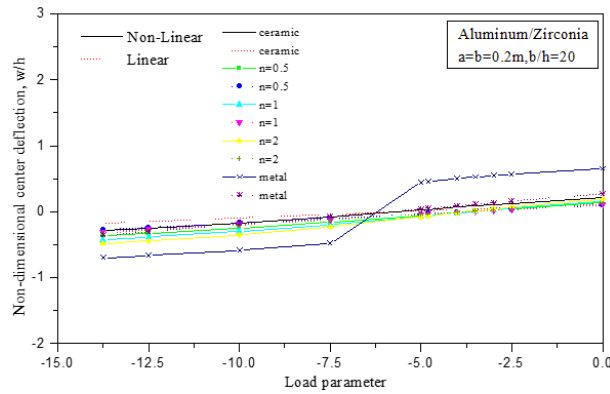


Fig. 7 Variation of the plate central deflection under combined uniform load and temperature field in case of linear and nonlinear analysis

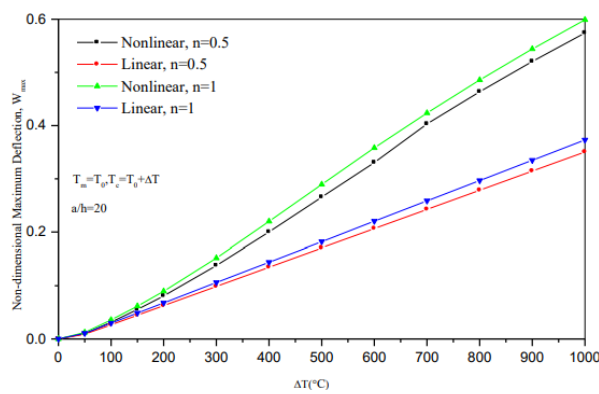


Fig. 8 Non-dimensional deflection versus thermal load

Fig. 4 represents the variation of the temperature across the FGM plate for various values of the volume fraction exponent n . it should be noted the temperature in the FGM plates is always greater

than found in fully ceramic or fully metallic plates. Fig. 5 shows non-dimensional central deflection of the FGM plate under load parameter for various values of volume fraction exponent in case of linear analysis and nonlinear analysis. Generally, it is observed that linear analysis overestimates the central deflection. Also, it is observed that the largest difference between linear and the nonlinear analysis is found in case of fully metal plate. Fig. 6 shows the non-dimensional central deflection of the plate in terms of the mechanical load with temperature field through the thickness of the plate. It should be noted that the central deflection for plate with graded material is greater than that of homogenous plate (ceramic or metal). This is due to the effect of the thermal conductivity on the deflection where in case of homogenous plate the thermal conductivity has no effect on the deflection, while in case of graded plate; the deflection is dependent on the thermal conductivity. Also, it is expected that the central deflection of fully metallic plate is greater than fully ceramic one. This is because the metal has a higher coefficient of thermal expansion than ceramic. In addition, graded plate tends to has downward deflection for higher mechanical pressure.

Variation of the plate central deflection under combined uniform load and temperature field is presented in Fig. 7. One can observe that also in this case of loading the linear analysis overestimates the central deflection especially in case of fully metallic plate. In addition to that, when only thermal load is applied, the deflection of fully metallic plate has the largest positive value which means that the plate has upward deflection. A comparison of linear and non-linear analysis for non-dimensional center deflection of FGM plates subjected to thermal loading is displayed in Fig. 8. Two values of power law index, n , 0.5 and 1 are considered. The figure show that the non-linear theory predicts greater deflections than linear theory. It must be emphasized that when only thermal load is existing, the use of linear analysis may result in great errors.

Figs. 9 and 10 show the non-dimensional axial stress through the thickness of the plate under uniform loading in case of linear and nonlinear analysis, respectively. It is seen that under the application of the pressure loading, the stress are compressive at the top surface and tensile at the bottom surface. For the different volume fraction exponents chosen, the plate corresponding to $n=2$ yielded the maximum compressive stress at the top surface. This is the ceramic rich surface. Note that the ceramics are weaker in tension than in the compression.

Fig. 9 shows the non-dimensional central deflection of FGM plate under thermal loading in case of linear and nonlinear analysis. By comparing the linear and nonlinear predictions, it is observed that grater values are predicted by the nonlinear analysis compared to linear analysis, which means that under thermal loading the linear analysis underestimates the central deflection. Figs. 10, 11 and 12 show, respectively, the linear and nonlinear plots of the axial stress through the thickness of the plate under uniform loading of $10^4 N/m^2$. For fully metal or fully ceramic plate, the axial stress distribution is linear through the thickness for both linear and nonlinear analysis but with higher magnitude for linear analysis.

Also, for linear analysis, the axial stress for different volume fractions is null at the mid-plane, while the zero-stress location for the nonlinear analysis is dependent on the volume fraction value.

It is noted also that, for the linear analysis of graded plate, the axial stress at the top surface is same for different volume fractions profile. The same observation is noticed at the bottom surface. However, the later observation is not valid for the nonlinear case of analysis.

In terms of stress magnitude, it should be noted that, the stress magnitude for the linear analysis is greater than that predicted by the nonlinear analysis. But for both cases, the magnitude of the compression stress at the top surface is always greater than the tensile stress magnitude at the bottom surface, for graded FGM plate. Figs. 11 and 12 illustrate the distribution of axial stress

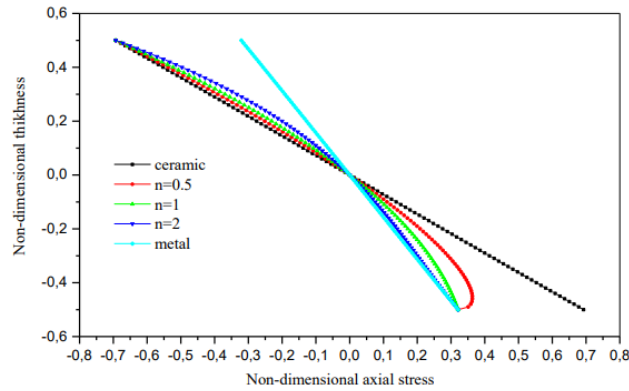


Fig. 9 Axial stress through the thickness of the plate under uniform loading of $-1 \times 10^4 \text{ N/m}^2$ in case of linear analysis

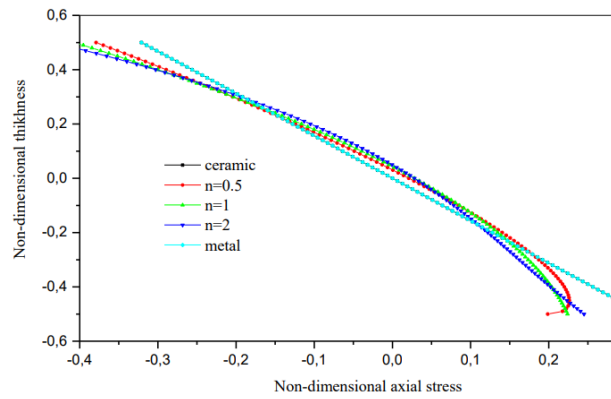


Fig. 10 Axial stress through the thickness of the plate under uniform loading of $-1 \times 10^4 \text{ N/m}^2$ in case of nonlinear analysis

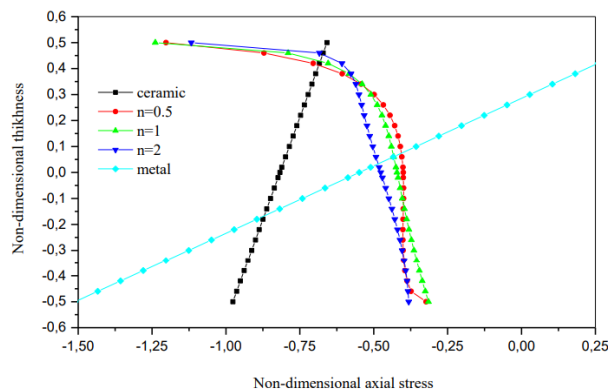


Fig. 11 Non-dimensional axial stresses in a simply supported square FGM plate under uniform loading of $-1 \times 10^4 \text{ N/m}^2$ and temperature field (aluminum zirconia)- Non-linear analysis

through the thickness of FGM plate, according to linear and nonlinear theory under both mechanical and thermomechanical loadings for magnitude of transverse load $100 \times 10^4 \text{ N/m}^2$. It is

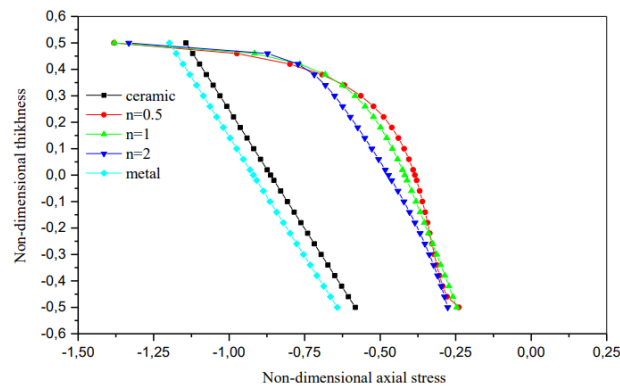


Fig. 12 Non-dimensional axial stresses in a simply supported square FGM plate under uniform loading of $-1 \times 10^4 \text{ N/m}^2$ and temperature field (aluminum zirconia)- linear Analysis

seen that for Fig. 11, the nature of the profile changes drastically for the metallic plate, and the magnitude of the compressive stress increases for FGM plates. Again, except for the ceramic plate, the stress profiles are close to each other, for the graded plates. Note that the stresses in the latter case are again compressive but with a higher magnitude, and this is because of the elastic strain which is different between the total strain and the thermal strain. Fig. 12 shows the FGM plate corresponding to $n=2$ experiences the maximum compressive stress at the top surface and the metallic and ceramic plates experience the maximum tensile stress at the bottom surface.

4. Conclusions

Theoretical formulation models based on the new third-order shear deformation theory with four variables is presented in this paper to carry out a nonlinear bending analysis of FGM plates. The formulation accounts for the thermo-mechanical coupling and Von-Karman type of geometric non-linearity. The material properties are assumed to be graded in the thickness direction according to a simple power-law distribution in terms of the volume fractions of the constituents. The concept of minimal energy method is used to obtain the solution.

It is found that the basic response of the plates that correspond to properties intermediate to that of the metal and the ceramic, does not necessarily lie in between that of the ceramic and metal.

The non-dimensional deflection was found to reach a minimum at a volume fraction index that depends on the properties and the ratio of the constituents. In the absence of thermal loading, the response of the graded plates is intermediate to that of the metal and ceramic plates. This is not the case when both thermal and mechanical loads are applied. This behavior is found to be true irrespective of boundary conditions. Thus, the gradients in material properties play an important role in determining the response of the FGM plates. Additionally, the numerical results show that the non-linearity effect on the plate responses is significant. An improvement of the present formulation will be considered in the future work to consider other type of materials (Akgöz and Civalek 2011, Daouadji *et al.* 2016, Mahapatra *et al.* 2016abc, Lal *et al.* 2017, Daouadji 2017, Mehar *et al.* 2017 and 2018, Hirwani *et al.* 2018, Patle *et al.* 2018, Katariya *et al.* 2018, Behera and Kumari 2018, Akbaş 2018 and 2019, Mehar and Panda 2019, Katariya and Panda 2019ab, Panjehpour *et al.* 2018, Ayat *et al.* 2018, Hussain and Naeem 2019, Sharma *et al.* 2019, Dash *et al.* 2019).

References

- Ahmed, A. (2014), "Post buckling analysis of sandwich beams with functionally graded faces using a consistent higher order theory", *Int. J. Civil Struct. Environ.*, **4**(2), 59-64.
- Akavci, S.S. (2016), "Mechanical behavior of functionally graded sandwich plates on elastic foundation", *Compos. Part B*, **96**, 136-152. <https://doi.org/10.1016/j.compositesb.2016.04.035>.
- Akbaş, Ş.D. (2017), "Nonlinear static analysis of functionally graded porous beams under thermal effect", *Coupled Syst. Mech.*, **6**(4), 399-415. <https://doi.org/10.12989/csm.2017.6.4.399>.
- Akbaş, Ş.D. (2018), "Nonlinear thermal displacements of laminated composite beams", *Coupled Syst. Mech.*, **7**(6), 691-705. <https://doi.org/10.12989/csm.2018.7.6.691>.
- Akbaş, Ş.D. (2019), "Forced vibration analysis of functionally graded sandwich deep beams", *Coupled Syst. Mech.*, **8**(3), 259-271. <http://doi.org/10.12989/csm.2019.8.3.259>.
- Akgöz, B. and Civalek, O. (2011), "Nonlinear vibration analysis of laminated plates resting on nonlinear two-parameters elastic foundations", *Steel Compos. Struct.*, **11**(5), 403-421. <https://doi.org/10.12989/scs.2011.11.5.403>.
- Aldousari, S.M. (2017), "Bending analysis of different material distributions of functionally graded beam", *Appl. Phys. A*, **123**(4), 296. <https://doi.org/10.1007/s00339-017-0854-0>.
- Avcar, M. (2019), "Free vibration of imperfect sigmoid and power law functionally graded beams", *Steel Compos. Struct.*, **30**(6), 603-615. <https://doi.org/10.12989/scs.2019.30.6.603>.
- Avcar, M. and Alwan, A.S. (2017), "Free vibration of functionally graded Rayleigh beam", *Int. J. Eng. Appl. Sci.*, **9**(2), 127-127. <http://dx.doi.org/10.24107/ijeas.322884>.
- Avcar, M. and Mohammed, W.K.M. (2018), "Free vibration of functionally graded beams resting on Winkler-Pasternak foundation", *Arab. J. Geosci.*, **11**(10), 232. <https://doi.org/10.1007/s12517-018-3579-2>.
- Ayat, H., Kellouche, Y., Ghrici, M. and Boukhatem, B. (2018), "Compressive strength prediction of limestone filler concrete using artificial neural networks", *Adv. Comput. Des.*, **3**(3), 289-302. <https://doi.org/10.12989/acd.2018.3.3.289>.
- Bakhti K., Kaci A., Bousahla A.A., Houari M.S.A., Tounsi A. and Adda Bedia E.A., (2013), "Large deformation analysis for functionally graded carbon nanotube-reinforced composite plates using an efficient and simple refined theory", *Steel Compos. Struct.*, **14**(4), 335-347. <http://dx.doi.org/10.12989/scs.2013.14.4.335>.
- Behera, S. and Kumari, P. (2018), "Free vibration of Levy-type rectangular laminated plates using efficient zig-zag theory", *Adv. Comput. Des.*, **3**(3), 213-232. <https://doi.org/10.12989/acd.2018.3.3.213>.
- Bensaid, I., Bekhadda, A., Kerboua, B. and Abdelmadjid, C. (2018), "Investigating nonlinear thermal stability response of functionally graded plates using a new and simple HSDT", *Wind Struct.*, **27**(6), 369-380. <https://doi.org/10.12989/was.2018.27.6.369>.
- Civalek, O. (2017), "Free vibration of carbon nanotubes reinforced (CNTR) and functionally graded shells and plates based on FSDT via discrete singular convolution method", *Compos. B Eng.*, **111**, 45-59. <https://doi.org/10.1016/j.compositesb.2016.11.030>.
- Daouadji, T.H. (2017), "Analytical and numerical modeling of interfacial stresses in beams bonded with a thin plate", *Adv. Comput. Des.*, **2**(1), 57-69. <https://doi.org/10.12989/acd.2017.2.1.057>.
- Daouadji, T.H., Benferhat, R. and Adim, B. (2016), "Bending analysis of an imperfect advanced composite plates resting on the elastic foundations", *Coupled Syst. Mech.*, **5**(3), 269-283. <https://doi.org/10.12989/csm.2016.5.3.269>.
- Dash, S., Mehar, K., Sharma, N., Mahapatra, T.R. and Panda, S.K. (2019), "Finite element solution of stress and flexural strength of functionally graded doubly curved sandwich shell panel", *Earthq. Struct.*, **16**(1), 55-67. <https://doi.org/10.12989/eas.2019.16.1.055>.
- Eltaher, M.A., Alshorbagy, A.E. and Mahmoud, F.F. (2013), "Determination of neutral axis position and its effect on natural frequencies of functionally graded macro/nanobeams", *Compos. Struct.*, **99**, 193-201. <https://doi.org/10.1016/j.compstruct.2012.11.039>.

- Ghayesh, M.H. and Farokhi, H. (2018), "Bending and vibration analyses of coupled axially functionally graded tapered beams", *Nonlin. Dyn.*, **91**(1), 17-28. <https://doi.org/10.1007/s11071-017-3783-8>.
- Hadji, L., Meziane, M., Abdelhak, Z., Daouadji, T.H. and Adda Bedia, E.A. (2016), "Static and dynamic behavior of FGM plate using a new first shear deformation plate theory", *Struct. Eng. Mech.*, **57**(1), 127-140. <https://doi.org/10.12989/sem.2016.57.1.127>.
- Hirwani, C.K., Panda, S.K. and Patle, B.K. (2018), "Theoretical and experimental validation of nonlinear deflection and stress responses of an internally debonded layer structure using different higher-order theories", *Acta Mechanica*, **229**(8), 3453-3473. <https://doi.org/10.1007/s00707-018-2173-8>.
- Hussain, M. and Naeem, M.N. (2019), "Rotating response on the vibrations of functionally graded zigzag and chiral single walled carbon nanotubes", *Appl. Math. Modell.*, **75**, 506-520. <https://doi.org/10.1016/j.apm.2019.05.039>.
- Kaci, A., Bakhti, K., Hebali, H., Tounsi, A. and Adda Bedia, E.A. (2013a), "Mathematical solution for nonlinear cylindrical bending of sigmoid functionally graded plates", *J. Appl. Mech. Tech. Phys.*, **54**(1), 124-131. <https://doi.org/10.1134/S002189441301015X>.
- Kaci, A., Belakhdar, K., Tounsi, A. and Adda Bedia, E.A. (2014), "Nonlinear cylindrical bending analysis of exponential functionally graded plates with variable thickness", *Steel Compos. Struct.*, **16**(4), 339-356. <http://dx.doi.org/10.12989/scs.2014.16.4.339>.
- Kaci, A., Draiche, K., Zidi, M., Houari, M.S.A. and Tounsi, A. (2013b), "An efficient and simple refined theory for nonlinear bending analysis of functionally graded sandwich plates", *J. Appl. Mech. Tech. Phys.*, **54**(5), 847-856. <https://doi.org/10.1134/S0021894413050180>.
- Kar, V.R. and Panda, S.K. (2015), "Nonlinear flexural vibration of shear deformable functionally graded spherical shell panel", *Steel Compos. Struct.*, **18**(3), 693-709. <https://doi.org/10.12989/scs.2015.18.3.693>.
- Kar, V.R. and Panda, S.K. (2016a), "Nonlinear thermomechanical deformation behaviour of P-FGM shallow spherical shell panel", *Chin. J. Aeronaut.*, **29**(1), 173-183.
- Kar, V.R. and Panda, S.K. (2016b), "Nonlinear thermomechanical behavior of functionally graded material cylindrical/hyperbolic/elliptical shell panel with temperature-dependent and temperature-independent properties", *J. Pressure Vessel Technol.*, **138**(6), 061202. <https://doi.org/10.1115/1.4033701>.
- Katariya, P. and Panda, S. (2019a), "Numerical evaluation of transient deflection and frequency responses of sandwich shell structure using higher order theory and different mechanical loadings", *Eng. Comput.*, **35**(3), 1009-1026. <https://doi.org/10.1007/s00366-018-0646-y>.
- Katariya, P. and Panda, S. (2019b), "Frequency and deflection responses of shear deformable skew sandwich curved shell panel: A finite element approach", *Arab. J. Sci. Eng.*, **44**(2), 1631-1648. <https://doi.org/10.1007/s13369-018-3633-0>.
- Katariya, P., Hirwani, C.K. and Panda, S. (2018), "Geometrically nonlinear deflection and stress analysis of skew sandwich shell panel using higher-order theory", *Eng. Comput.*, **35**(2), 467-485. <https://doi.org/10.1007/s00366-018-0609-3>.
- Kolahchi, R., Zarei, M.Sh., Hajmohammad, M.H. and Naddaf Oskouei, A. (2017), "Visco-nonlocal refined Zigzag theories for dynamic buckling of laminated nanoplates using differential cubature-Bolotin methods", *Thin-Wall. Struct.*, **113**, 162-169. <https://doi.org/10.1016/j.tws.2017.01.016>.
- Lal, A., Jagtap, K.R. and Singh, B.N. (2017), "Thermo-mechanically induced finite element based nonlinear static response of elastically supported functionally graded plate with random system properties", *Adv. Comput. Des.*, **2**(3), 165-194. <https://doi.org/10.12989/acd.2017.2.3.165>.
- Li, D., Deng, Z., Chen, G., Xiao, H. and Zhu, L. (2017), "Thermomechanical bending analysis of sandwich plates with both functionally graded face sheets and functionally graded core", *Compos. Struct.*, **169**, 29-41. <https://doi.org/10.1016/j.compstruct.2017.01.026>.
- Mahapatra, T.R., Kar, V. and Panda, S. (2016a), "Large amplitude bending behaviour of laminated composite curved panels", *Eng. Comput.*, **33**(1), 116-138. <https://doi.org/10.1108/EC-05-2014-0119>.
- Mahapatra, T.R., Panda, S.K. and Kar, V. (2016b), "Geometrically nonlinear flexural analysis of hygro-thermo-elastic laminated composite doubly curved shell panel", *Int. J. Mech. Mater. Des.*, **12**(2), 153-171. <https://doi.org/10.1007/s10999-015-9299-9>.
- Mahapatra, T.R., Panda, S.K. and Kar, V. (2016c), "Nonlinear flexural analysis of laminated composite

- panel under hygro-thermo-mechanical loading—A micromechanical approach”, *Int. J. Comput. Meth.*, **13**(3), 1650015. <https://doi.org/10.1142/S0219876216500158>.
- Mantari J.L., Oktem A.S. and Guedes Soares C. (2012), “Bending response of functionally graded plates by using a new higher order shear deformation theory”, *Compos. Struct.*, **94**(2), 714-723. <https://doi.org/10.1016/j.compstruct.2011.09.007>.
- Mehar, K. and Panda, S.K. (2019), “Theoretical deflection analysis of multi-walled carbon nanotube reinforced sandwich panel and experimental verification”, *Compos. Part B Eng.*, **167**, 317-328. <https://doi.org/10.1016/j.compositesb.2018.12.058>.
- Mehar, K., Panda, S.K. and Patle, B.K. (2017), “Thermoelastic vibration and flexural behavior of FG-CNT reinforced composite curved panel”, *Int. J. Appl. Mech.*, **9**(4), 1750046. <https://doi.org/10.1142/S1758825117500466>.
- Mehar, K., Panda, S.K. and Patle, B.K. (2018), “Stress, deflection, and frequency analysis of CNT reinforced graded sandwich plate under uniform and linear thermal environment: A finite element approach”, *Polym. Compos.*, **39**(10), 3792-3809. <https://doi.org/10.1002/pc.24409>.
- Miyamoto Y., Kaysser W.A., Rabin B.H., Kawasaki A. and Ford R.G., (1999), *Functionally Graded Materials, Design, Processing and Applications*, Kluwer Academic Publishers, Netherlands.
- Mohammadzadeh, B., Choi, E. and Kim, D. (2019), “Vibration of sandwich plates considering elastic foundation, temperature change and FGM faces”, *Struct. Eng. Mech.*, **70**(5), 601-621. <https://doi.org/10.12989/sem.2019.70.5.601>.
- Nguyen-Xuan H., Tran L.V., Thai C.H., Kulasegaram S. and Bordas S.P.A., (2014), “Isogeometric analysis of functionally graded plates using a refined plate theory”, *Compos. Part B Eng.*, **64**, 222-234. <https://doi.org/10.1016/j.compositesb.2014.04.001>.
- Panjehpour, M., Loh, E.W.K. and Deepak, T.J. (2018), “Structural insulated panels: State-of-the-Art”, *Trends Civ. Eng. Architect.*, **3**(1) 336-340. <https://doi.org/10.32474/TCEIA.2018.03.000151>.
- Patle, B.K., Hirwani, C.K., Singh, R.P. and Panda, S.K. (2018), “Eigenfrequency and deflection analysis of layered structure using uncertain elastic properties – a fuzzy finite element approach”, *Int. J. Approx. Reason.*, **98**, 163-176. <https://doi.org/10.1016/j.ijar.2018.04.013>.
- Ramos, I.A., Mantari, J.L., Pagani, A. and Carrera, E. (2016), “Refined theories based on non-polynomial kinematics for the thermoelastic analysis of functionally graded plates”, *J. Therm. Stresses*, **39**(7), 835-853. <https://doi.org/10.1080/01495739.2016.1189771>.
- Reddy, J.N. (2000), “Analysis of functionally graded plates”, *Int. J. Numer. Meth. Eng.*, **47**(1-3), 663-684. [https://doi.org/10.1002/\(SICI\)1097-0207\(20000110/30\)47:1/3<663::AID-NME787>3.0.CO;2-8](https://doi.org/10.1002/(SICI)1097-0207(20000110/30)47:1/3<663::AID-NME787>3.0.CO;2-8).
- Shahsavari, D., Shahsavari, M., Li, L. and Karami, B. (2018), “A novel quasi-3D hyperbolic theory for free vibration of FG plates with porosities resting on Winkler/Pasternak/Kerr foundation”, *Aerosp. Sci. Technol.*, **72**, 134-149. <https://doi.org/10.1016/j.ast.2017.11.004>.
- Sharma, N., Lalepalli, A.K., Hirwani, C.K., Das, A. and Panda, S.K. (2019), “Optimal deflection and stacking sequence prediction of curved composite structure using hybrid (FEM and soft computing) technique”, *Eng. Comput.*, 1-11. <https://doi.org/10.1007/s00366-019-00836-8>.
- Siddiqui, F. (2015), “Extended higher order theory for sandwich plates of arbitrary aspect ratio”, Ph.D. Thesis, Georgia Institute of Technology, Georgia, Atlanta, U.S.A.
- Sobhy, M. (2013), “Buckling and free vibration of exponentially graded sandwich plates resting on elastic foundations under various boundary conditions”, *Compos. Struct.*, **99**, 76-87. <https://doi.org/10.1016/j.compstruct.2012.11.018>.
- Talha, M. and Singh, B.N. (2011), “Nonlinear mechanical bending of functionally graded material plates under transverse loads with various boundary conditions”, *Int. J. Model. Simul. Sci. Comput.*, **2**(2), 237-258. <https://doi.org/10.1142/S1793962311000451>.
- Thai, H.T. and Choi, D.H. (2013), “A simple first-order shear deformation theory for the bending and free vibration analysis of functionally graded plates”, *Compos. Struct.*, **101**, 332-340. <https://doi.org/10.1016/j.compstruct.2013.02.019>.
- Thai, H.T. and Kim, S.E. (2013), “A simple higher-order shear deformation theory for bending and free vibration analysis of functionally graded plates”, *Compos. Struct.*, **96**, 165-173.

<https://doi.org/10.1016/j.compstruct.2012.08.025>.

Tornabene, F., Brischetto, S., Fantuzzi, N. and Baccocchi, M. (2016), "Boundary conditions in 2D numerical and 3D exact models for cylindrical bending analysis of functionally graded structures", *Shock Vib.*, 114-129. <http://dx.doi.org/10.1155/2016/2373862>.

Tuma, J.J. (1970), *Engineering Mathematics Handbook, Definitions, Theorems, Formulas, Tables*, McGraw-Hill Inc., New York, U.S.A.

Yang, J. and Shen, H.S. (2003), "Nonlinear bending analysis of shear deformable functionally graded plates subjected to thermo-mechanical loads under various boundary conditions", *Compos. Part B*, **34**(2), 103-115. [https://doi.org/10.1016/S1359-8368\(02\)00083-5](https://doi.org/10.1016/S1359-8368(02)00083-5).

CC